The Plant Cell, Vol. 31: 1913–1929, August 2019, www.plantcell.org © 2019 ASPB.

Pectin Methylesterases Modulate Plant Homogalacturonan Status in Defenses against the Aphid *Myzus persicae*[OPEN]

Christian Silva-Sanzana,[a] Jonathan Celiz-Balboa,[a] Elisa Garzo,[b] Susan E. Marcus,[c] Juan Pablo Parra-Rojas,[a] Barbara Rojas,[a] Patricio Olmedo,[a] Miguel A. Rubilar,[a] Ignacio Rios,[a] Rodrigo A. Chorbadjian,[d] Alberto Fereres,[b] Paul Knox,[d] Susana Saez-Aguayo,[a,1] and Francisca Blanco-Herrera[a,e,1]

[a] Centro de Biotecnología Vegetal, Facultad de Ciencias de la Vida, Universidad Andres Bello, Santiago 8370186, Chile
[b] Instituto de Ciencias Agrarias, Consejo Superior de Investigaciones Científicas, Madrid 28006, Spain
[c] Centre for Plant Sciences, Faculty of Biological Sciences, University of Leeds, Leeds LS2 9JT, United Kingdom
[d] Facultad de Agronomía e Ingeniería Forestal, Pontificia Universidad Católica de Chile, Santiago 7820436, Chile
[e] Millennium Institute for Integrative Biology, Santiago 7500565, Chile

ORCID IDs: 0000-0003-2556-1106 (C.S.-S.); 0000-0002-7135-0193 (J.C.-B.); 0000-0001-8626-5832 (E.G.); 0000-0002-5495-5684 (S.E.M.); 0000-0002-3111-0603 (J.P.P.-R.); 0000-0002-0697-0185 (B.R.); 0000-0001-8152-8381 (P.O.); 0000-0002-1711-7606 (M.A.R.); 0000-0002-6528-381X (I.R.); 0000-0001-8664-1770 (R.A.C.); 0000-0001-6012-3270 (A.F.); 0000-0002-9231-6891 (P.K.); 0000-0002-2250-6454 (S.S.-A.); 0000-0002-7497-9907 (F.B.-H.)

Because they suck phloem sap and act as vectors for phytopathogenic viruses, aphids pose a threat to crop yields worldwide. Pectic homogalacturonan (HG) has been described as a defensive element for plants during infections with phytopathogens. However, its role during aphid infestation remains unexplored. Using immunofluorescence assays and biochemical approaches, the HG methylesterification status and associated modifying enzymes during the early stage of Arabidopsis (*Arabidopsis thaliana*) infestation with the green peach aphid (*Myzus persicae*) were analyzed. Additionally, the influence of pectin methylesterase (PME) activity on aphid settling and feeding behavior was evaluated by free choice assays and the Electrical Penetration Graph technique, respectively. Our results revealed that HG status and HG-modifying enzymes are significantly altered during the early stage of the plant-aphid interaction. Aphid infestation induced a significant increase in total PME activity and methanol emissions, concomitant with a decrease in the degree of HG methylesterification. Conversely, inhibition of PME activity led to a significant decrease in the settling and feeding preference of aphids. Furthermore, we demonstrate that the PME inhibitor AtPMEI13 has a defensive role during aphid infestation, since *pmei13* mutants are significantly more susceptible to *M. persicae* in terms of settling preference, phloem access, and phloem sap drainage.

INTRODUCTION

Phytophagous insects have developed different strategies to extract nutrients from plants to complete their life cycle, resulting in a direct impairment of host health and performance. Of the phytophagous insects that affect commercial crops, aphids have a greater impact due to the nutrient losses caused by colonies draining plants and promoting saprophytic fungal growth, thus significantly decreasing crop yields (Östman et al., 2003; Dedryver et al., 2010). Moreover, viruses transmitted by aphids are the most relevant risk factor for the target crop. Indeed, aphids function as vectors for ~50% of the 700 known insect-borne viruses (Hooks and Fereres, 2006; Dedryver et al., 2010). Consequently, aphids are one of the most costly pests in terms of pesticide treatments (Murray et al., 2013).

The aphid feeding process starts when the stylet penetrates the host and then moves toward the phloem through intercellular pathways, such as cell wall matrices, middle lamellae, and gas spaces, until sieve elements are reached (Kimmins, 1986; Tjallingii and Esch, 1993). Most cells along the stylet pathway are briefly punctured (typically for 5–10 s), but the stylets are always withdrawn from the cells and then continue along the intercellular route until sieve elements are found (Tjallingii and Esch, 1993).

Intercellular cell wall polysaccharides are a main component of the intercellular stylet pathway. These macromolecules share common features among vascular plants and consist of cellulose microfibrils anchored to the cell membrane, cross-linked by and embedded in matrices of hemicellulose and pectic polymers (Ridley et al., 2001; Wolf and Greiner, 2012). In this context, homogalacturonan (HG) has been found to participate in different plant developmental and defensive processes (Ridley et al., 2001; Gramegna et al., 2016). HG is a homopolymer of galacturonic acid (GalA) residues, which can be methylesterified at C-6 and may carry acetyl groups on O-2 and O-3 (Ridley et al., 2001). According to the current model of HG synthesis, it has been established that HGs are synthesized in the Golgi apparatus in a highly methylesterified state and then secreted into the cell wall (Ibar and Orellana, 2007). In the cell wall, the methylesterification status may be modified by the action of pectin methylesterases (PMEs), which

[1] Address correspondence to susana.saez@unab.cl and mblanco@unab.cl.
The author responsible for distribution of materials integral to the findings presented in this article in accordance with the policy described in the Instructions for Authors (www.plantcell.org) is: Francisca Blanco-Herrera (mblanco@unab.cl).
[OPEN]Articles can be viewed without a subscription.
www.plantcell.org/cgi/doi/10.1105/tpc.19.00136

remove the methylester groups (EC 3.1.1.11). In turn, these reactions of HG demethylesterification are regulated by the proteinaceous PME inhibitors (PMEIs) (Hothorn et al., 2004; Caffall and Mohnen, 2009; Saez-Aguayo et al., 2013; Levesque-Tremblay et al., 2015).

The degree and pattern of HG methylesterification are key factors influencing the mechanical properties of cell walls, and hence in controlling plant development (Peaucelle et al., 2008; Levesque-Tremblay et al., 2015). In fact, depending on the methylesterification degree, HG domains can be directed into different fates: (1) polymer breakdown by polygalacturonases (PGs; EC 3.2.1.15) and pectate lyase (PL; EC 4.2.2.2), causing cell wall loosening, and (2) ionic cross-linking with other demethylesterified HG chains through calcium ion bridges, creating the so-called "egg box" structures leading to cell wall stiffening and reduced matrix porosity (Braccini et al., 1999; Willats et al., 2001; Levesque-Tremblay et al., 2015).

HG modification and degradation are important factors during the attack of pathogens or phytophagous insects possessing cell wall-degrading enzymes such as PMEs, PGs, and PLs as virulence factors (Cantu et al., 2008; Malinovsky et al., 2014). The evidence linking HG to the defensive responses of plants includes the broad spectrum of pathogen resistance or susceptibility phenotypes that are created by altering HG-modifying enzymes in different plant species (Cantu et al., 2008). Although the evidence relating to HG metabolism during aphid feeding is limited, it is thought that the presence of HG-modifying enzymes such as PMEs and PGs, in the saliva of aphids, could facilitate stylet penetration through the intercellular matrix (McAllan and Adams, 1961; Dreyer and Campbell, 1987; Ma et al., 1990). Additionally, by exploring the transcriptional profiles of Arabidopsis (*Arabidopsis thaliana*) plants attacked by different pathogens and phytophagous insects, De Vos et al. (2005) found that the *PECTIN METHYLESTERASE13* (*AtPMEI13*) gene was specifically upregulated during *Myzus persicae* feeding yet was unchanged during the interaction with other attackers studied. Despite this valuable information, there still exists a lack of detailed mechanistic understanding about the role of HG during plant-aphid interactions.

The focus of the present work was to characterize the dynamics of HG and its modifying enzymes during the early stage of aphid infestation and how these changes could influence the aphid settling and feeding behavior. To this end, the globally distributed aphid *M. persicae* and Arabidopsis were used as the plant-aphid interaction model. Here, we show that during early aphid infestation, total PME activity and methanol emission increase with a concomitant decrease in the degree of HG methylesterification. Exogenous inhibition of total PME activity leads to a significant decrease in aphid settling preference in wild-type Col-0 plants. Furthermore, by exploiting the results obtained by De Vos et al. (2005), the inhibitory activity of AtPMEI13 and its defensive role during aphid infestation were isolated and characterized. Due to the marked preference of *M. persicae* to settle on *pmei13* plants, concomitant with longer phloem sap ingestions on these mutants compared with the wild-type genotypes, it has been demonstrated that AtPMEI13 is a resistance factor during aphid colonization in Arabidopsis.

RESULTS

Determination of Early Infestation Stage during *M. persicae*-Arabidopsis Interaction

Prior to the experiments and analysis, in order to determine the time scales of the early infestation stages, the proper sampling time for the experiments was established. We decided to establish as the early aphid infestation stage the time that aphids took to perform the first sustained phloem ingestion from the first contact with the Arabidopsis leaf (aphid landing). To this, we used the Electrical Penetration Graph (EPG) technique, which creates distinct fluctuating voltage patterns referred to as EPG waveforms, which in turn has been experimentally related to different feeding processes or activities performed by the insect, in this case the aphid *M. persicae* (Figure 1A).

The EPG results showed that wingless adult *M. persicae* aphids settled on wild-type leaves and achieved the first sustained phloem ingestion after 271.2 ± 34.8 min (4.5 ± 0.5 h) from landing (Figure 1B). Thus, considering that aphids took ~5 h to perform the first sustained phloem ingestion (and adding 1 h to cover possible variations), we established as an early infestation stage the first 6 h of plant aphid interaction, and based on this timing, further experiments were done. Additionally, EPG analysis revealed that after the first host penetration, performed 4.2 min after landing, host tissues were probed by aphids ~35 times (35 probes), and within these probing events, *M. persicae* performed an average of 145 membrane punctures, visualized as potential drops (Figures 1A and 1B). Moreover, during the first 360 min (6 h), *M. persicae* spent just 85.1 min in nonprobing activities (i.e., with their stylets out of the host plant) (Figure 1B). Therefore, this confirmed that aphids perform an exhaustive examination by constantly probing the host tissues during the early infestation stage (6 h of plant-aphid interaction).

Early Stage of Aphid Infestation Increases Total PME Activity, Methanol Emissions, and Abundance of Demethylesterified HG

Considering that PME activity and the HG methylesterification status have been described as defense-related elements during pathogen attack (Cantu et al., 2008; Osorio et al., 2008; Raiola et al., 2011; Bethke et al., 2014), it was decided to measure the total PME activity and its consequent effects on the HG methylesterification degree and methanol emissions (Figure 2A) during the early stage of plant-aphid interaction. Our results showed that total PME activity increased ~20% in aphid-infested leaves of Arabidopsis with respect to the control plants (i.e., noninfested; Figure 2B). Consequently, the degree of methylesterification of HG decreased significantly by 19% (Figure 2C), concomitant with a threefold increase in the methanol emissions in the aphid-infested plants compared with the control condition (Figure 2D).

To visualize the cell wall modifications that occurred as a result of the increase in PME activity, immunofluorescence assays on infected and control Arabidopsis leaves were performed. The immunofluorescence assays that were done to visualize the HG methylesterification status, in situ, support the

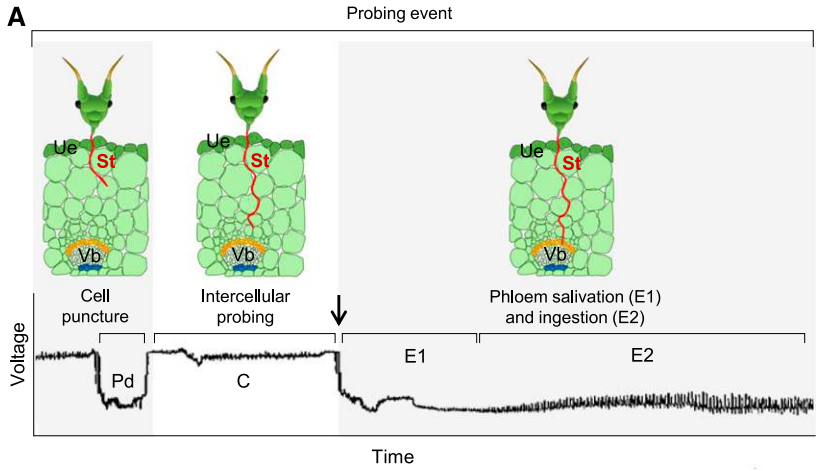

B

	Duration (min)	
Sequential variables	Mean	SE
Time from start of EPG to 1st sustained phloem ingestion (> 10 min) (time for host acceptance)	271.2	34.8
Time from start of EPG to first probe	4.2	1.1
Non-sequential variables	Mean	SE
Number of probes	35.2	3.0
Duration of non-probing	85.1	10.2
Number of potential drops	145.1	15.2

Figure 1. Determination of Sampling Time for Early Aphid Infestation Stage.

EPG was performed to evaluate the feeding behavior of *M. persicae* using Arabidopsis (wild-type Col-0) as a host with the aim of determining the proper sampling time related to the early infestation stage.

(A) Schematic representation of the biological activities of the aphid stylet inside the host plant and its corresponding EPG waveform. The arrow points to the potential drop related to the stylet entry into the sieve elements. C, intercellular probing; E1, phloem salivation; E2, phloem ingestion; Pd, cell puncture (potential drop); St, stylet; Ue, upper epidermis; Vb, vascular bundle.

(B) EPG variables analyzed to define the timing of the early aphid infestation stage. Mean and SE were calculated from $n = 20$ (20 independent EPG recordings).

results obtained in Figures 2B. and 2C The LM19 monoclonal antibody, which targets the demethylesterified domains of HG, showed a doubling of the signal in the parenchyma tissue and lower epidermis of infested leaves, with respect to the control condition (Figure 3; Supplemental Figures 1). and 2 Additionally, some replicates with LM19 antibody revealed HG demethylesterification zones localized close to aphid bodies and stylets (Supplemental Figure 1), suggesting that HG modifications could be occurring as a consequence of stylet penetration through the pectic matrix. On the other hand, a significant 30% reduction in the signal of the LM20 antibody, which recognizes highly methylesterified HG, was observed in the aphid-infested leaves compared with the noninfested plants (Figure 3; Supplemental Figure 3). Additionally, HG epitopes were measured by enzyme-linked immunosorbent assay (ELISA); however, no differences were detected during aphid infestation by this method (Supplemental Figure 4). Therefore, these results showed that early aphid infestation induced an increase in the total PME activity, with the consequent demethylesterification of HG and methanol release.

Early Stage of Aphid Infestation Increases the Calcium Cross-Linked HG and Alters the Total PL Activity

Once HG chains are demethylesterified in cell walls, they may be directed to two different fates: (1) polymer breakdown by PGs and/or PLs or (2) interact ionically with other demethylesterified HG chains through calcium bridges, creating the so-called egg box structures (Figure 4A; Braccini et al., 1999; Willats et al., 2001). Then, as the early *M. persicae* infestation process induces HG deesterification, which of these two subsequent steps (PG/PL breakdown or egg box arrangement) could be occurring in early aphid-infested plants was investigated. To achieve this, total PG and PL activities were measured. The results revealed that the total PG activity remains unchanged (Figure 4B), concomitant with a significant increase in total PL activity (Figure 4C), in the aphid-infested plants with respect to the control condition.

Since the other possible fate of demethylesterified HG is the ion cross-linking, we visualized these epitopes by using the monoclonal antibody 2F4. Interestingly, it was found that the egg box arrangement of HG is significantly more abundant in infested

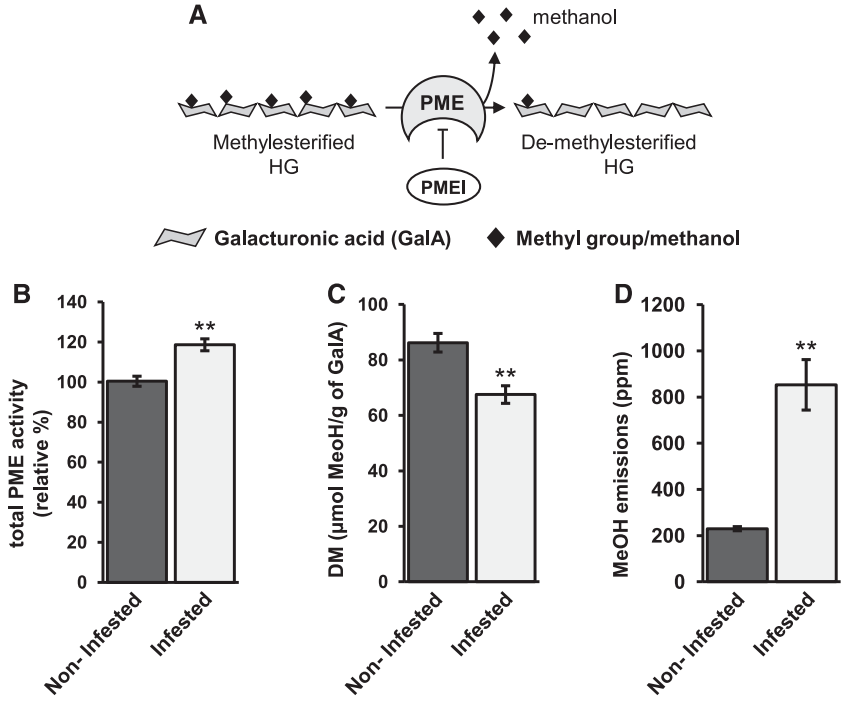

Figure 2. Early Plant-Aphid Interaction Increases Global PME Activity and Decreases the Degree of HG Methylesterification.

(A) Schematic representation of the HG demethylesterification process. PME is catalyzed by HG demethylesterification, and their activity is regulated by their proteinaceous inhibitor (PMEIs).

(B) Total PME activity measured after 6 h of *M. persicae*-Arabidopsis interaction with 4-week-old wild-type Col-0 plants. Total protein extracts from rosette leaves of wild-type Col-0 plants were used to measure global PME activity. Values are expressed as relative PME activity and normalized to the average wild-type Col-0 activity (noninfested). Error bars represent SE from $n = 3$ (three individual plants).

(C) Degree of methylesterification (DM) after 6 h of *M. persicae*-Arabidopsis interaction. Error bars represent SE from $n = 3$ (three individual plants).

(D) Methanol (MeOH) emissions measured after 6 h of *M. persicae*-Arabidopsis interaction with 4-week-old wild-type Col-0 plants by full evaporation headspace gas chromatography. Values correspond to ppm of methanol in 1 µL of collected transpiration vapor. Error bars represent SE from $n = 4$ (four individual plants).

(B) to **(D)** Asterisks represent significant differences determined by Student's *t* test (**, $P < 0.005$).

plants, since a significant tripling in the signal of 2F4 antibody was measured mainly in the lower epidermis and parenchyma tissue of the aphid-infested leaves compared with the control condition (Figures 4D and 4E; Supplemental Figure 5). This suggests that, during early *M. persicae* infestation, changes in HG structure lead to an increase in the abundance of both demethylesterified and ion cross-linked HG.

Exogenous Modulation of PME Activity and Methanol Emissions Influence the Aphid Settling Preference

The above results revealed that HG methylesterification status is significantly altered during the early plant-aphid interaction (Figures 2 and 3; Supplemental Figures 1 to 3). However, we cannot distinguish whether these HG alterations correspond to a defensive mechanism of the host plant or to the consequences of the aphid infestation/feeding process. In order to gain an insight into this question, it was decided to investigate how different levels of PME activity of the host plant could influence the aphid behavior in terms of settling preference.

The first approach was to exogenously modulate the total PME activity of wild-type Col-0 plants and then subject these plants to a free choice assay, which reveals the preference of the aphids to settle on the most suitable host to establish a new colony (Poch et al., 1998). This was achieved by infiltrating one group of plants with 1 mg/mL epigallocatechin gallate (EGCG; Sigma-Aldrich), which has been described as a specific chemical inhibitor of global PME activity (Lewis et al., 2008). Then, a second group of plants was infiltrated with 15 units/mL orange peel PME (Sigma-Aldrich; Figure 5A). After 1 h of the infiltration procedure, treated plants plus a water-infiltrated control group (mock) were subjected to the free choice assay. The results show that treatment with the chemical PME inhibitor EGCG resulted in ~10% reduction in total PME activity (Figure 5B) concomitant with a 2.7-fold reduction of methanol emissions (Figure 5D) compared with the infiltration control (mock). On the other hand, infiltration with the commercial orange peel PME cocktail increased the total PME activity by 15% (Figure 5B) compared with the mock-infiltrated plants, while methanol emissions showed no differences between both conditions (Figure 5D). Free choice assays on these treated plants

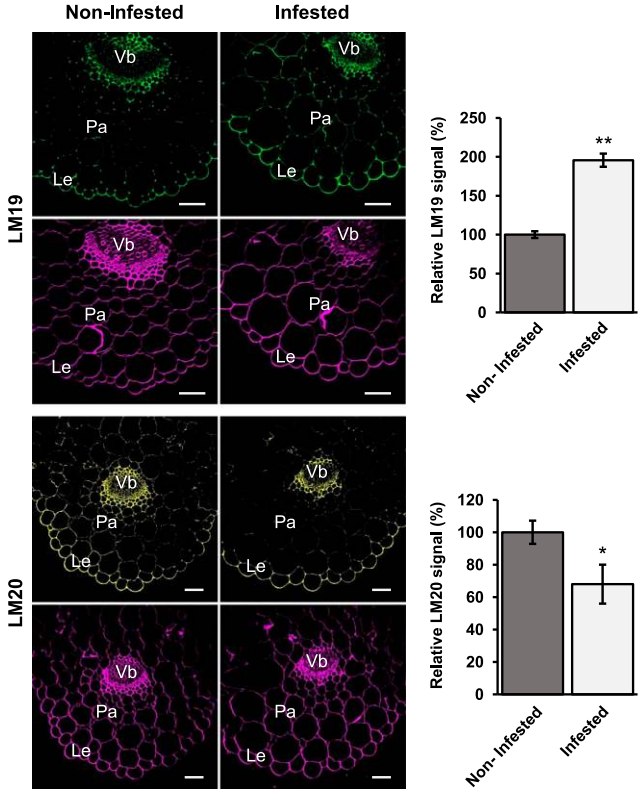

Figure 3. Early Aphid Infestation Increases the Abundance of Demethylesterified HG Epitopes.

Representative transverse sections of 4-week-old wild-type Col-0 Arabidopsis leaves were immunolabeled with LM19 and LM20 monoclonal antibodies to target demethylesterified HG (green) and highly methylesterified HG (yellow), respectively. Calcofluor White was applied to stain all cell walls (magenta). The images show closeups of the lower epidermis and parenchyma surrounding the main vascular bundle of leaves of noninfested and infested plants. Le, lower epidermis; Pa, parenchyma; Vb, vascular bundle. Bars = 50 μm. The graphs at right show the relative fluorescence signal of each antibody. Values were normalized with respect to the noninfested condition. Error bars represent the SE obtained from four biological replicates (four leaves from different plants, from different culture batches). Asterisks represent significant differences determined by Student's *t* test (*, $P < 0.05$ and **, $P < 0.005$).

showed no significant differences in aphid preference when compared with the increased PME activity group of plants (PME infiltrated) with the control condition (mock; Figure 5C). Interestingly, a significant reduction in aphid settling was observed for the reduced PME activity plants (EGCG infiltrated), since only 20% of the total aphid population preferred those plants as host, compared with 38% and 42% of the aphid population that preferred to settle on mock-treated and orange peel PME-treated plants, respectively (Figure 5C).

Moreover, it is known that methanol is a critical volatile defense signal emitted during phytophagous insect feeding (Baldwin et al., 2006; von Dahl et al., 2006), and considering that our results show increased methanol emissions in aphid-infested plants (Figure 2D), it was decided to investigate how methanol emissions could influence the host settling preference of *M. persicae*. To accomplish this and based on methanol emissions from infested plants, which averaged 0.09% (v/v) (900 ppm; Figure 2D), a methanol solution of 0.1% (v/v) was prepared to infiltrate wild-type Col-0 leaves, and then these plants were subjected to an aphid free choice assay using water-infiltrated plants as controls (mock). As shown in Figure 5E, the results revealed that aphids significantly prefer to settle on methanol-infiltrated plants, since 60% of the total aphid population chose those plants as host compared with the 40% of insects that chose the mock plants. These results suggest that both exogenous modulation of PME activity and methanol emission in Arabidopsis leaves could influence the *M. persicae* settling preference. However, considering that the infiltration procedure could lead to unknown changes in the plant physiology and consequently alter the aphid behavior, a second approach was designed in order to determine the influence of the PME activity over the settling behavior of aphids.

PMEI13 Possesses in Vitro and in Vivo Inhibitory Activity of PMEs, and *pmei13* Mutant Lines Are More Susceptible to *M. persicae* Settling

Expression analysis using a microarray published by De Vos et al. (2005) showed that a PME inhibitor (PMEI13) is specifically upregulated during *M. persicae* infestation of Arabidopsis. Considering this finding, the potential role of PMEI13 during the plant-aphid interaction was evaluated. Two T-DNA insertional mutant lines were identified in the locus *At5g62360/PMEI13* and were designated as *pmei13-1* (background Col-0) and *pmei13-2* (background WS4; Supplemental Figure 6A). Expression analysis using RT-PCR and RT-qPCR were done on *pmei13-1* and *pmei13-2* mutant plants. Amplification of the full-length coding sequence of *PMEI13* in both *pmei13-1* and *pmei13-2* mutant lines confirmed that both mutants are knockdown lines, with decreases of 65.5 and 57.1% in *PMEI13* transcript accumulation in comparison with their corresponding wild-type genotypes, respectively (Supplemental Figures 6B and 6C). Then, in order to characterize the PME-inhibiting capacity of PMEI13, the inhibitory effect of recombinant PMEI13 on global PME activity of wild-type plants by using a gel diffusion assay was determined, as described by Saez-Aguayo et al. (2013, 2017). The results presented in Supplemental Figure 6D show that the induced bacterial culture containing the recombinant PMEI13 (PMEI13x6 his + IPTG) has 30% and 23% less global PME activity than cultures containing the empty vector (EV + IPTG) and the noninduced PMEI13 construct (PMEI13x6 his – IPTG), respectively. Thus, these results confirm that PMEI13 is an inhibitor of pectin methylesterase activity.

To confirm the in vivo inhibitor activity of PMEI13 in Arabidopsis, total PME activity was measured in 4-week-old *pmei13-1* and *pmei13-2* plants. The results show that both *pmei13* mutant lines possess higher total PME activity compared with the wild-type genotypes. *pmei13-1* showed 14% more PME activity compared with wild-type Col-0, while *pmei13-2* exhibited 11% more PME activity compared with wild-type WS4 (Supplemental Figure 7A). These significant increases in total PME activity observed in *pmei13* mutants were consistent with the increased

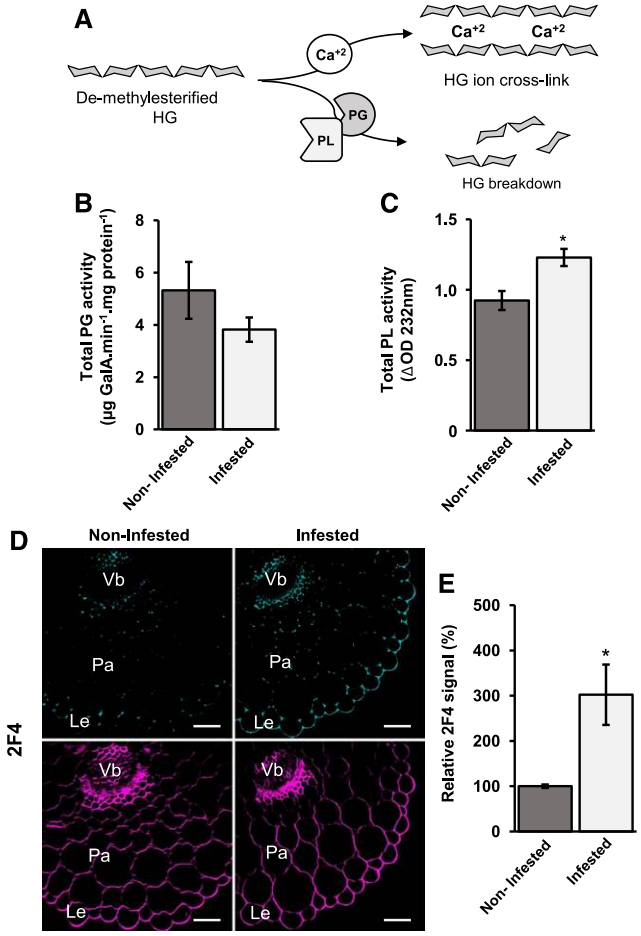

Figure 4. Early Stage of Aphid Infestation Increases the Calcium Cross-Linked HG and Alters the Total PL Activity.

(A) Schematic representation of the two possible fates of demethylesterified HGs: (1) to form a stable ion cross-linked structure with other demethylesterified HG blocks via calcium, or (2) to be degraded by the hydrolytic action of PGs or PLs.
(B) Total PG activity measured after 6 h of *M. persicae*-Arabidopsis interaction. Error bars represent SE from $n = 3$ (three individual plants).
(C) Total PL activity measured after 6 h of *M. persicae*-Arabidopsis interaction. Error bars represent SE from $n = 4$ (four individual plants).
(D) Representative transverse sections of 4-week-old wild-type Col-0 Arabidopsis leaves were immunolabeled with 2F4 monoclonal antibody to target ion cross-linked HG (cyan). Calcofluor White was applied to stain all the cell walls (magenta). Images show closeups of the lower epidermis and parenchyma surrounding the main vascular bundle of leaves of noninfested and infested plants. Le, lower epidermis; Pa, parenchyma; Vb, vascular bundle. Bars = 50 µm.
(E) Relative fluorescence signal of 2F4 antibody. Values are normalized with respect to the noninfested condition. Error bars represent the SE obtained from three biological replicates (three leaves from different plants, from different culture batches).
Asterisks represent significant differences determined by Student's *t* test (*, $P < 0.05$).

abundance of demethylesterified HG epitopes (Figures 6A and 6B; Supplemental Figures 8 and 9), concomitant with significant decreases of 7 and 11% in the degree of methylesterification of *pmei13-1* and *pmei13-2*, respectively, compared with their wild-type genotypes (Supplemental Figure 7B). In addition, both mutant lines possess higher methanol emissions compared with wild-type genotypes. *pmei13-1* showed a significant increase of ~72 ppm related to wild-type Col-0, while *pmei13-2* showed an increase of ~164 ppm when compared with wild-type WS4 (Supplemental Figure 7C).

Given that *PMEI13* specifically responds to *M. persicae* attack (De Vos et al., 2005) and that *pmei13* lines basally possess higher levels of total PME activity with respect to the wild-type genotypes (Supplemental Figure 7A), it was decided to further investigate these mutants. This was done to evaluate the influence of PME activity over aphid settling and feeding behavior. Thus, this represents an alternative approach to the exogenously manipulated PME levels, and it is not subject to the possible side effects of infiltration procedures, since PME activity is basally and endogenously modulated in *pmei13* mutant lines compared with wild-type genotypes. Hence, once characterized, the role of PMEI13 in plant defense in terms of aphid settling preference was investigated. Both mutant lines (*pmei13-1* and *pmei13-2*) were subjected to a dual choice assay against their respective wild-type backgrounds. Figure 6C shows that both *pmei13* mutant plants are significantly more preferred by *M. persicae*. Approximately 71% of the total aphid population chose the *pmei13-1* mutant line to settle, compared with 29% of the population that chose the wild-type Col-0 genotype. This aphid behavior was observed 2 h after the start of the assay and showed no significant fluctuation during the 24 h of the experiment (Figure 6C). In the case of *pmei13-2*, 62% of the total aphid population preferred to settle on this mutant line and 38% of insects chose the wild-type WS4 as host (Figure 6C), showing no further variations during the 24 h of the assay. Thus, loss of function of AtPMEI13 resulted in a significant susceptibility to aphids settling on Arabidopsis, therefore confirming the influence of the plant PME activity over the settling behavior of *M. persicae*.

The *pmei13* Mutant Plants Are More Susceptible to Phloem Nutrient Drainage by *M. persicae*

HG and its modifying enzymes have been described as an element controlling cell wall rheology (Braccini et al., 1999; Willats et al., 2001) and defense response sensing and triggering (Cantu et al., 2008; Lionetti et al., 2017). Thus, taking into account that *pmei13* lines possess increased PME activity and a lower degree of HG methylesterification (Supplemental Figures 7A and 7B), it was decided to investigate how these alterations could influence the aphid feeding behavior. By using EPG technology, the aphid feeding variables associated with mechanical or chemical traits of host plants were analyzed. This could determine the global host resistance or susceptibility to aphid colonization. The results showed that significant differences between genotypes were found in feeding activities related to the phloem ingestion phase and phloem accessibility (Tables 1 and 2). In the case of *pmei13-1*, aphids spent more than twice as long (155.2 min) sucking nutrients from the phloem (waveform E2) compared with wild-type Col-0 (66.8 min; Table 1). Sustained phloem sap ingestions (E2 waveform > 10 min) were 2.6 times longer when *M. persicae* fed on *pmei13-1* (145.5 min) instead of wild-type Col-0 (54.6 min), and the mean duration of the longest phloem ingestions was 3.4 times longer on the mutant genotype (119.5 min) compared with its wild

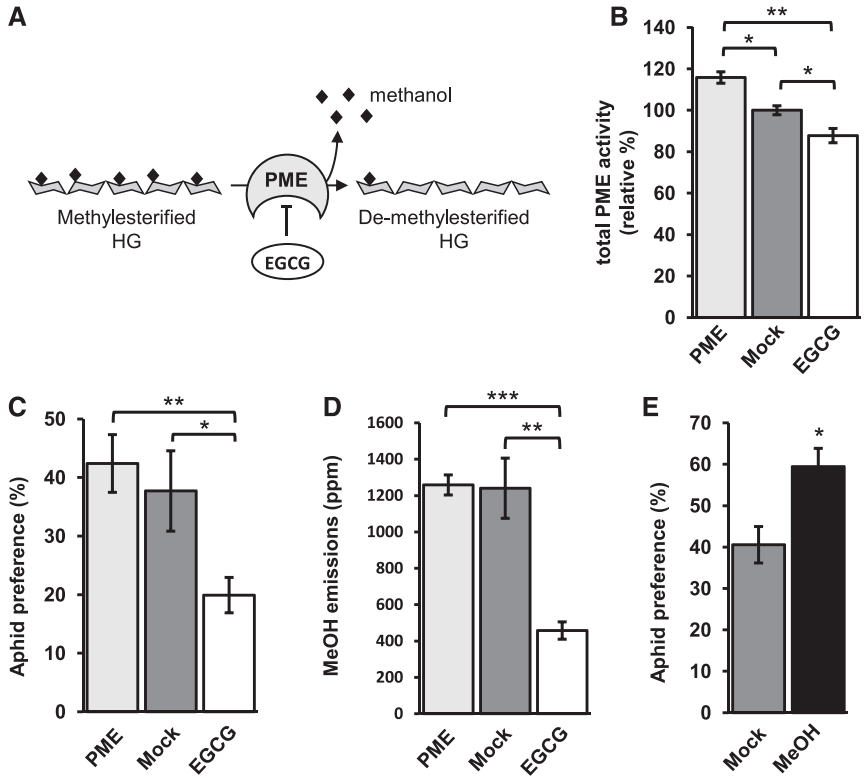

Figure 5. Exogenous Modulation of Total PME Activity Alters Aphid Host Choice Behavior.

(A) Schematic representation of PME activity and methanol release. A commercial PME cocktail and EGCG were used to increase and to inhibit global PME activity, respectively. Infiltration of methanol was performed to mimic the induction of HG demethylation during early aphid feeding.

(B) Total PME activity exogenously modified in wild-type Col-0 plants by infiltrating leaves with commercial orange peel PME or the PME activity inhibitor EGCG. Total protein extracts from infiltrated leaves were used to measure PME activity. Values are expressed as relative PME activity and normalized to the average value in noninfiltrated wild-type Col-0 leaves (Mock). Error bars represent SE from $n = 3$ (three individual plants).

(C) Choice assay performed to evaluate the aphid settling preference on plants with exogenously altered PME activity. Thirty aphids were released equidistantly from orange peel PME- and EGCG-infiltrated plants and allowed to freely choose their host. After 24 h, the total number of aphids per plant was counted. Error bars represent SE from five independent choice tests.

(D) Methanol (MeOH) emissions measured on plants with exogenously modified PME activity by full evaporation headspace gas chromatography. Values correspond to ppm of methanol in 1 μL of collected transpiration vapor. Error bars represent SE from $n = 4$ (four individual plants).

(E) Choice assay performed to evaluate the aphid settling preference on plants infiltrated with methanol (0.1%, v/v). Thirty aphids were released equidistantly from mock- and methanol-treated plants and allowed to freely choose their host. After 24 h, the total number of aphids per plant was counted. Error bars represent SE from five independent choice tests.

(B) to **(E)** Asterisks represent significant differences determined by Student's *t* test (*, $P < 0.05$; **, $P < 0.005$; and ***, $P < 0.001$).

type (35.9 min), whereas the nonphloem phase was significantly shorter in *pmei13-1* mutants (304.3 min) compared with wild-type Col-0 (405.6 min) (Table1), which is consistent, since a longer nonphloem phase directly implies that aphids spend more time on other activities, different from phloem salivation or ingestion. No significant differences were detected for other probing/feeding activities, such as intercellular probing (waveform C), xylem ingestion (waveform G), and cell puncturing (waveform pd). Moreover, *M. persicae* was able to perform the first host probe significantly faster on *pmei13-1* (1.9 min) than on wild-type Col-0 (4.5 min). Similarly, it took significantly less time for aphids to perform the first phloem ingestion when fed on *pmei13-1* (157.0 min) compared with wild-type Col-0 (226.4 min; Table 1).

In the case of *pmei13-2*, the longest phloem ingestions were significantly longer in the mutant genotype (154.7 min) compared with wild-type WS4 (89.0 min), while other parameters related to phloem ingestion (waveform E2) showed no significant differences (Table 2). However, the duration of sustained phloem ingestion (E2 waveform > 10 min) showed a clear tendency ($P = 0.080$) to be longer when aphids were fed on *pmei13-2* (199.7 min) compared with wild-type WS4 (147.0 min). The same phenomenon was observed for the total duration of the phloem ingestion phase (waveform E2), since this variable tended to be longer for *pmei13-2* (211.6 min) than for wild-type WS4 (161.1 min; $P = 0.093$). Moreover, as with *pmei13-1*, significantly less time was needed by aphids to perform the first phloem ingestion when fed on *pmei13-2* (106.1 min) compared with wild-type WS4 (159.9 min; Table 2). Likewise, aphids required significantly less time to perform the first sustained phloem ingestion (E2 > 10 min) on *pmei13-2* (163.9 min) compared with wild-type WS4 (234.1 min;

Table 2). No significant differences were found for other probing/feeding activities (waveforms np, C, pd, G, F, and E1).

DISCUSSION

Early Aphid Infestation Induces an Increase in PME Activity, Methanol Emissions, and Demethylesterified HG

HG and its modifying enzymes have been associated with plant defense mechanisms from bacterial and fungal pathogen attacks; however, its defensive role during aphid infestation remains uncertain. Here, the dynamics of HG and its modifying enzymes were described during the early aphid infestation stage (6 h), and the defensive role of the Arabidopsis PME inhibitor (PMEI13) in terms of aphid settling and feeding behavior was characterized.

The results revealed that during the first 6 h of aphid infestation, the total PME activity increased significantly in infested Arabidopsis leaves, with a consequent increase in the abundance of demethylesterified HG and methanol release (Figure 2). It has been proposed that demethylesterification of HG is a key step to elicit an efficient defense response (Osorio et al., 2008). Conversely, the defense-eliciting activity of HG oligomers (oligogalacturonides) is

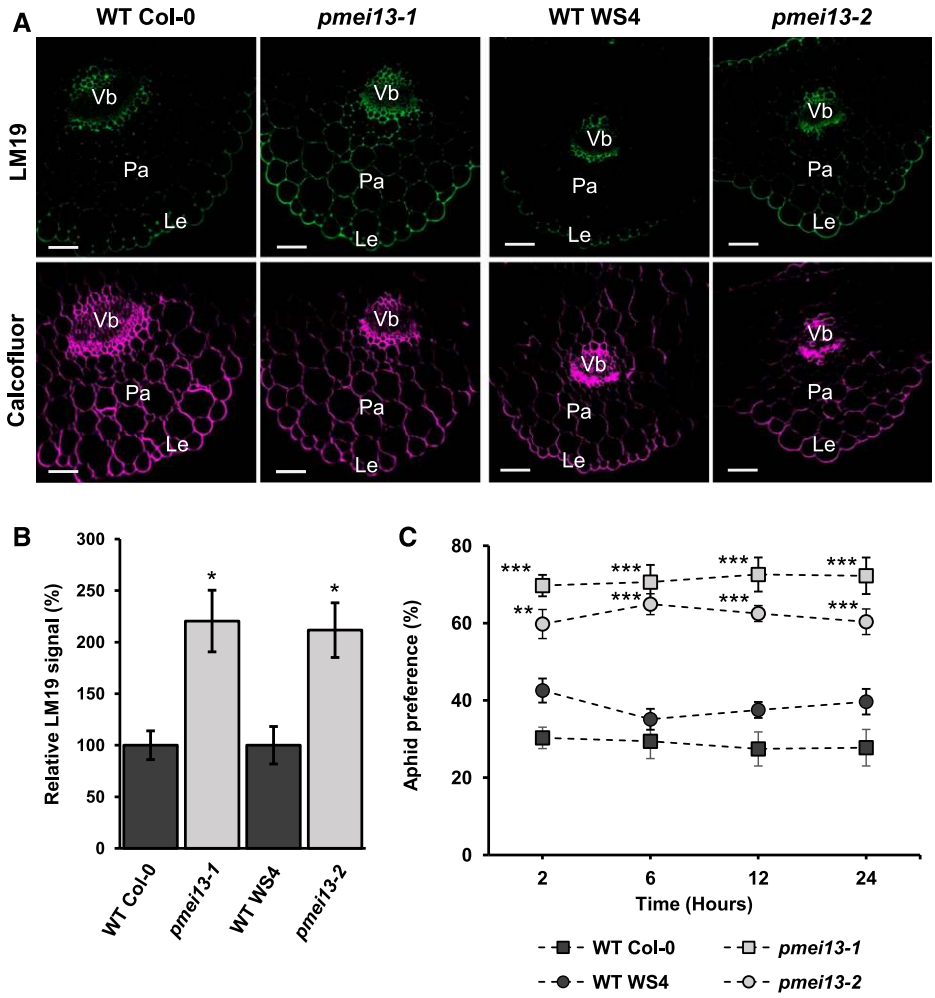

Figure 6. *pmei13* Mutants Possess Increased Abundance of Demethylesterified HG and Are More Susceptible to *M. persicae* Settling Compared with Wild-Type Genotypes.

(A) Representative transverse sections of 4-week-old wild-type Col-0, wild-type WS4, *pmei13-1*, and *pmei13-2* leaves were immunolabeled with LM19 monoclonal antibody to target demethylesterified HG (green). Calcofluor White was applied to stain all the cell walls (magenta). Le, lower epidermis; Pa, parenchyma; Vb, vascular bundle. Bars = 50 μm.

(B) Relative fluorescence signal of LM19 antibody. Values of *pmei13* mutant lines were normalized with respect to its respective wild-type genotypes. Error bars represent the SE obtained from three biological replicates (three leaves from different plants, from different culture batches).

(C) Choice assay performed to evaluate the aphid settling preference on *pmei13* mutant lines. Thirty aphids were released equidistantly from wild-type Col-0 and *pmei13-1* or from wild-type WS4 and *pmei13-2*. Aphids were allowed to freely choose their host, and the total number of aphids per plant was counted after 24 h. Error bars represent SE from five independent choice tests.

(B) to **(C)** Asterisks represent significant differences as determined by Student's *t* test (*, $P < 0.05$; **, $P < 0.005$; and ***, $P < 0.001$).

Table 1. *pmei13-1* Plants Are More Susceptible to Phloem Accessibility and Drainage by Aphid Feeding

Non-Sequential Variables	Genotype	Mean	SE	P
Total duration of np	Col-0	114.4	14.4	0.237
	pmei13-1	92.3	11.3	
Total probing time	Wild-type Col-0	365.6	14.4	0.257
	pmei13-1	387.2	11.3	
Total duration of C	Wild-type Col-0	219.2	11.9	0.158
	pmei13-1	191.5	17.2	
Total duration of pd	Wild-type Col-0	16.9	1.3	0.137
	pmei13-1	13.8	1.3	
Total duration of G	Wild-type Col-0	15.4	4.4	0.834
	pmei13-1	13.9	4.3	
Total duration of F	Wild-type Col-0	61.3	19.2	0.072
	pmei13-1	22.5	10.7	
Total duration of E1	Wild-type Col-0	3.9	0.6	0.435
	pmei13-1	4.0	1.0	
Total duration of E2	Wild-type Col-0	66.8	10.5	0.034*
	pmei13-1	155.2	26.5	
Duration of the longest E2	Wild-type Col-0	35.9	5.7	0.033*
	pmei13-1	119.5	26.3	
Duration of sustained E2	Wild-type Col-0	54.6	10.3	0.040*
	pmei13-1	145.5	27.2	
Total duration of E	Wild-type Col-0	70.6	10.6	0.030*
	pmei13-1	159.2	26.5	
Duration of nonphloematic phase	Wild-type Col-0	405.6	10.4	0.007**
	pmei13-1	304.3	26.5	
Sequential variables				
Time to first probe from start of EPG	Wild-type Col-0	4.5	1.2	0.050*
	pmei13-1	1.9	0.4	
Time from first probe to first E2	Wild-type Col-0	226.4	27.7	0.044*
	pmei13-1	157.0	27.6	
Time from first probe to first sustained E2	Wild-type Col-0	287.2	32.8	0.268
	pmei13-1	232.8	33.1	

EPG recordings during 8 h were performed in order to analyze the feeding behavior profile of adult *M. persicae* aphids on *pmei13-1* and wild-type Col-0. Mean and SE were calculated from $n = 20$ (20 independent EPG recordings). Asterisks represent significant differences determined by the Mann-Whitney *U* test (*, $P < 0.05$; **, $P < 0.005$). C, intercellular probing; E1, phloem salivation; E2, phloem ingestion; F, stylet derail; G, xylem ingestion; np, nonprobing; pd, cell punctures (potential drop).

significantly reduced when their degree of methylesterification increases (Jin and West, 1984; Navazio et al., 2002). Therefore, taking into account the results and the previous evidence, the HG demethylesterification process that is taking place during the first 6 h of *M. persicae*-Arabidopsis interaction could represent part of the elicitation of an efficient defense response against the insect. However, a detailed study of the defense pathways, its dynamics, and related phytohormones is needed to support this hypothesis. With respect to the increased methanol emissions on aphid-infested plants (Figure 2D), it is described that this molecule acts as a volatile signal recognized by plants but also by phytophagous insects (Komarova et al., 2014). For example, methanol emitted by mechanically wounded tobacco (*Nicotiana tabacum*) leaves (methanol emitter plants) acts as a signaling molecule that is involved in plant-to-plant communication, promoting antibacterial resistance on nonwounded neighboring plants (methanol receivers) (Dorokhov et al., 2012). Additionally, PME-overexpressing tobacco plants possessing higher levels of methanol emissions compared with the wild-type genotype showed a dramatic increase in resistance to different phytophagousinsects such as caterpillars, aphids, and whiteflies (Dixit et al., 2013). However, the study performed by von Dahl et al. (2006) showed that by applying methanol to plants (in quantities that mimic the caterpillar feeding), the performance of the attacking larvae increases significantly. This antecedent is in part similar to the results shown in Figure 5E, where methanol-treated plants (at a concentration that mimics the aphid-infested plants) were significantly more attractive to aphids, which is consistent with the aphid settling preference observed for PME- or EGCG-treated plants, since plants with more methanol emissions are significantly more preferred by *M. persicae* (Figures 5C to 5E). These results provide a potential insight for future studies aiming to understand methanol signaling during aphid infestation.

Early Aphid Infestation Promotes the Increase in Demethylesterified and Ion Cross-Linked HG Forms

After demethylesterification, HG can be cleaved by PG/PL or cross-linked through calcium ions (Braccini et al., 1999; Willats et al., 2001). Considering that early aphid infestation promotes the demethylesterification of HG in Arabidopsis (Figure 2; Supplemental Figures 1 to 3), which of the two fates is taking place for HG in

Table 2. *pmei13-2* Plants Are More Susceptible to Phloem Accessibility and Drainage by Aphid Feeding

Non-sequential variables	Genotype	Mean	SE	P
Total duration of np	WS4	83.6	12.0	0.364
	pmei13-2	66.6	8.7	
Total probing time	Wild-type WS4	396.4	12.0	0.364
	pmei13-2	413.4	8.7	
Total duration of C	Wild-type WS4	194.4	13.4	0.496
	pmei13-2	179.3	13.8	
Total duration of pd	Wild-type WS4	13.8	1.1	0.982
	pmei13-2	13.9	1.3	
Total duration of G	Wild-type WS4	18.5	6.1	0.193
	pmei13-2	7.1	2.8	
Total duration of F	Wild-type WS4	21.0	7.7	0.648
	pmei13-2	15.7	6.7	
Total duration of E1	Wild-type WS4	3.4	0.3	0.803
	pmei13-2	3.4	0.4	
Total duration of E2	Wild-type WS4	161.1	22.9	0.093
	pmei13-2	211.6	19.4	
Duration of the longest E2	Wild-type WS4	89.0	16.4	0.019*
	pmei13-2	154.7	19.9	
Duration of sustained E2	Wild-type WS4	147.0	23.9	0.080
	pmei13-2	199.7	20.3	
Total duration of E	Wild-type WS4	164.5	22.9	0.097
	pmei13-2	215.0	19.1	
Duration of nonphloematic phase	Wild-type WS4	315.5	22.9	0.097
	pmei13-2	265.0	19.1	
Sequential variables				
Time to first probe from start of EPG	Wild-type WS4	2.3	0.6	0.51
	pmei13-2	2.9	0.8	
Time from first probe to first E2	Wild-type WS4	159.9	20.4	0.028*
	pmei13-2	106.1	12.5	
Time from first probe to first sustained E2	Wild-type WS4	234.1	26.2	0.028*
	pmei13-2	163.9	22.4	

EPG recordings during 8 h were performed in order to analyze the feeding behavior profile of adult *M. persicae* aphids on *pmei13-2* and wild-type WS4. Mean and SE were calculated from $n = 20$ (20 independent EPG recordings). Asterisks represent significant differences determined by the Mann-Whitney *U* test (*, $P < 0.05$). C, intercellular probing; E1, phloem salivation; E2, phloem ingestion; F, stylet derail; G, xylem ingestion; np, nonprobing; pd, cell punctures (potential drop).

aphid-infested leaves was investigated. The results show that both demethylesterified and ion cross-linked HG epitopes increased in aphid-infested leaves, while highly methylesterified HG decreased (Figures 2, 3, 4D, and 4E; Supplemental Figures 1 to 5).

Although quantification of epitope abundance in cell wall extracts by ELISA showed no difference between infested and noninfested leaves (Supplemental Figure 4), immunofluorescence experiments revealed that the HG demethylesterification zones in aphid-infested leaves could be notably heterogeneous in pattern, distribution, and size. This probably depends on the time that an aphid spent in the same probing site (Supplemental Figure 1). Thus, altered HG from zones where aphids remained attached could be diluted with the rest of the nonprobed cell walls of the same infested leaves. Another possible explanation could be that the critical HG component that shows methylesterification differences between the treatments corresponds to the fractions solubilized by KOH and/or cellulose. In these cases, all methylesters were removed by the alkali treatment, and thus HG methylesterification cannot be assessed.

Concerning the influence that the different HG forms possess over the mechanical properties of the extracellular matrix, studies performed by atomic force microscopy have shown that demethylesterification of pectin contributes to an increase in the elasticity of meristematic cells in Arabidopsis (Peaucelle et al., 2011). On the other hand, calcium cross-linked HG has been associated with a decreased elasticity and increased stiffness through in vitro assays (Fraeye et al., 2010; Ngouémazong et al., 2012). Conversely, these results indicate that both HG forms (demethylesterified and ion cross-linked) increase in aphid-infested plants (Figures 3 and 4). It is not possible to argue with the influence of the mechanical properties of this HG form over the stylet penetration through the extracellular matrix, and further mechanical studies must be done to support this hypothesis. However, an interesting clue regarding this idea could be extracted from the EPG analysis, since it revealed that aphids reached the phloem significantly faster on *pmei13* mutants (Tables 1 and 2), which in turn possess a significantly lower basal degree of HG methylesterification compared with the wild-type genotypes (Supplemental Figure 7D).

Exogenous and Endogenous Modulations of Total PME Activity in Arabidopsis Influence the *M. persicae* Settling Preference

In order to understand the influence of PME activity over *M. persicae* settling behavior, the first approach was to exogenously

modulate the total PME activity by infiltrating a commercial PME cocktail and a chemical inhibitor of PME (EGCG) into wild-type Col-0 plants and then to expose these plants to a free choice assay with mock-infiltrated plants. The results of this experiment showed that aphids significantly preferred to settle on plants with higher levels of PME activity (PME infiltrated and mock) compared with plants with lower PME activity levels (EGCG infiltrated; Figure 5). However, it is important to mention that the EGCG inhibitor, exogenous PMEs (nonself PMEs), and methanol infiltration procedures could lead to unknown side effects on the physiological status of the infiltrated plants, which in turn could alter aphid behavior.

For this reason, the second approach was to obtain PME or PMEI mutant plants of Arabidopsis possessing different basal levels of PME activity compared with wild-type genotypes. It is known that PMEs and PMEIs correspond to large protein families in Arabidopsis, possessing 66 and 69 putative genes encoding for PMEs and PMEIs, respectively (Wolf et al., 2009). Additionally, the potential redundancy and promiscuity of the PMEI isogenes and the lack of information about their specific interacting PME partners (Wolf et al., 2009; Jolie et al., 2010; Sénéchal et al., 2015) hinder the investigation of their individual physiological roles. Fortunately, by exploring the transcriptional profiles of Arabidopsis attacked by different pathogens and phytophagous insects, De Vos et al. (2005) found that the *AtPMEI13* gene was specifically upregulated during *M. persicae* feeding. Once the genotype and phenotype characterization of *pmei13* lines was done (Supplemental Figures 6 to 9), both mutant lines (*pmei13-1* and *pmei13-2*) were subjected to a dual free choice assay against their respective wild-type genotypes (wild-type Col-0 and wild-type WS4), revealing that *M. persicae* significantly preferred to settle on *pmei13* plants (Figure 6C). Thus, aphids are significantly more attracted by *pmei13* plants, which possess higher PME activity levels, methanol emissions, and demethylesterified HG abundance.

The *pmei13* Plants Are More Susceptible to Phloem Access and Drainage by *M. persicae*

EPG assays have been used to dissect and identify the elements that compose the global susceptibility or resistance phenotypes of several plant species to different phloem feeder insects (Poch et al., 1998; Garzo et al., 2002; Klingler et al., 2005; Le Roux et al., 2008). Thus, in order to gain insights into the specific factors influenced by the lack of PMEI13 over aphid infestation performance, the complete probing and feeding behavior profile of *M. persicae* on *pmei13* mutant lines using the EPG technique (Tables 1 and 2) was evaluated. The results of this analysis showed that both *pmei13* mutant genotypes are significantly more susceptible than their respective wild type, in terms of phloem accessibility and phloem sap drainage by *M. persicae* (Tables 1 and 2).

The fact that the duration of the longest phloem ingestions was significantly greater in both *pmei13* mutants compared with their wild-type genotypes (Tables 1 and 2) allows us to suggest that a specific trait of the phloem cells or nutrient composition could be influenced by the loss of the inhibitory activity of AtPMEI13. It has been described that differences in the duration of phloem ingestions (waveform E2) can be caused by the presence of deterrent compounds or a clogging mechanism in the phloem (Harrewijn and Kayser, 1997; Klingler et al., 1998; Tjallingii, 2006; Zhang et al., 2011). In these cases, the duration of phloem salivation (waveform E1), which always precedes phloem ingestion (waveform E2), is significantly longer, since this feeding activity corresponds to an aphid mechanism to overcome the defensive elements of the host (Tjallingii, 2006; Peng and Walker, 2018). However, the EPG analysis showed no differences in phloem salivation (waveform E1) between *pmei13* and wild-type plants, and hence the existence of a phloem trait different from clogging systems or deterrent compound presence may be involved. In addition, *pmei13* plants exhibited a clear susceptibility in terms of phloem accessibility, since aphids took significantly less time to reach the phloem phase (waveform E) in both mutant lines (Tables 1 and 2). This result suggests the participation of a prephloem mechanism related to changes in the intercellular matrix rheology or anatomical variations that could hinder phloem access to stylets in wild-type genotypes. This hypothesis can be supported in part by the lower HG methylesterification degree of *pmei13* plants, which has been previously correlated with increased flexibility of cell walls in Arabidopsis (Peaucelle et al., 2011), hence stylet movement toward sieve elements could be less hindered in *pmei13* lines compared with wild-type genotypes.

Until now, due to the limited knowledge available, it has not been possible to understand the role of each member of the PMEI family during aphid infestation in Arabidopsis. However, by studying the feeding behavior profile of *M. persicae* in PMEI6 overexpresser plants (characterized in Saez-Aguayo et al., 2013), it was found that none of the feeding activities studied were altered compared with wild-type Col-0 (Supplemental Table 1). The first insights suggest that not all members of the PMEI family in Arabidopsis possess the same level of influence over the plant-aphid interaction as that observed with PMEI13. This is probably due to the interaction with specific PME partners expressed during aphid infestation.

METHODS

Plant Material and Growth Conditions

The Arabidopsis (*Arabidopsis thaliana*) wild-type Col-0 accession and the *pmei13-1* (Salk_035506) T-DNA mutant line were obtained from the ABRC (http://abrc.osu.edu/) using the SIGnAL Salk collection (Alonso et al., 2003). The wild-type WS4 and the *pmei13-2* (FLAG_58B07) mutant were obtained from the Versailles Arabidopsis Stock Center (http://publiclines.versailles.inra.fr/). Homozygous lines were identified by PCR using the primers indicated in Supplemental Table 2 using genomic DNA. Plants were grown in peat-vermiculite soil in a controlled environment chamber (21–26°C, photoperiod of 16 h of light/8 h of dark, 65% relative humidity, and cold white LED lamps providing 120 μmol m^{-2} s^{-1} light intensity).

Insect Growth Conditions and Infestation Treatment

Parthenogenetic colonies of the green peach aphid *Myzus persicae* were maintained on pesticide-free *Brassica oleracea* var *capitata* plants grown in peat moss substrate. Growth chambers were set to 25°C ± 2°C and 55 to 65% relative humidity. Fully expanded leaves of 4-week-old Arabidopsis (wild-type Col-0) plants were each infested with 20 wingless adult aphids. Aphids were confined on each fully expanded leaf using clip cages built with 300-μm sheer mesh. After 6 h of plant-aphid interaction, insects were

removed, and plant tissue was immediately frozen in liquid nitrogen and stored in −80°C containers. Noninfested plants were used as the control condition.

Expression Analysis

RNA extractions were performed using an RNeasy Plus Micro Kit (Qiagen). One microgram of total RNA was used as a template for first-strand cDNA synthesis with an oligo(dT) primer and SuperScript II (Thermo Fisher Scientific), according to the manufacturer's instructions. For RT-PCR analysis, the primers described in Supplemental Table 2 were used to amplify the entire coding sequence of *PMEI13* from single-stranded cDNA in wild-type Col-0, WS4, *pmei13-1*, and *pmei13-2* plants. The primers used to amplify *EF1aA4* were those described by (North et al., 2007). RT-qPCR was performed using the Fast EvaGreen qPCR Master Mix kit (Mx3000P; Stratagene). Reactions contained 1 μL of 1:2 diluted cDNA in a total volume of 10 μL. Reactions were performed using primers that had been previously tested for their efficiency rates and sensitivity in a cDNA dilution series. The quantification and normalization procedures were performed using the equation described by Saez-Aguayo et al. (2017). *EF1aA4* and *UBC9* were used as reference genes, and all primers used in this study are described in Supplemental Table 2.

Determination of total PME, PG, and PL Activities

For determination of global PME, PG, and PL total activities, total protein extracts were obtained by homogenizing 100 μg of tissue in 150 μL of extraction buffer (1 M NaCl, 0.2 M Na_2HPO_4, and 0.1 M citric acid, pH 6.5). The homogenates were incubated at 4°C for 1.5 h, cleared twice by centrifugation at 15,000*g* for 10 min at 4°C, and the supernatant recovered. Protein concentration was determined based on a BSA standard curve using a Pierce BCA Protein Assay Kit (Thermo Fisher Scientific).

Global PME activity was quantified by the radial gel diffusion assay. Equal quantities of protein (8 μg) were loaded into 5-mm-diameter wells on gels prepared with 0.1% (w/v) 85% esterified citrus fruit pectin (Sigma-Aldrich), 1% (w/v) agarose, 12.5 mM citric acid, and 50 mM Na_2HPO_4, pH 6.5. After incubation overnight at 28°C, plates were stained with 0.01% ruthenium red for 45 min and destained with distilled water. The total area of stained halos was measured using ImageJ software. Results were expressed as relative percentages with respect to the halo area measured in noninfested controls.

To determine global PG activity, an enzymatic reaction was performed by mixing 0.3 mL of reaction buffer (200 mM NaCl and 200 mM sodium acetate, pH 4.5), 400 μg of total protein extract in 0.1 mL of extraction buffer, and 0.3 mL of 1% (w/v) polygalacturonic acid. Reactions were started by incubation at 37°C for 60 min and finished by heating at 100°C for 5 min. To quantify reducing sugars produced by PG activity, 100 μL of DNS reagent (Sigma-Aldrich) was added to 100 μL of the reaction mix and heated at 100°C for 30 min. Tubes were ice chilled for 5 min, and 1 mL of distilled water was added. The formation of reducing groups was quantified against a standard curve of galacturonic acid (US Biological) and measured at 540 nm. PG activity was defined as the amount of enzyme required to produce 1 μg GalA h^{-1} mg^{-1} protein.

PL enzyme activity was determined as described by Uluisik et al. (2016) with minor modifications. Briefly, 50 μg of total protein extracts was incubated in a solution containing 0.12% (w/v) polygalacturonic acid, 30 mM Tris-HCl, pH 8.5, and 0.15 mM $CaCl_2$. The absorbance of products with double bonds released was measured at 232 nm in an initial time (T0) and after incubation at 30°C for 15 h (T15). Results are expressed as the change of absorbance between T15 and T0 at 232 nm.

Determination of Methanol Emissions by Full Evaporation Headspace Gas Chromatography

Stomatal vapor was collected by individually enclosing the Arabidopsis rosettes inside a 50-mL tube during 5 min at 60°C. The tubes were placed immediately on ice for 5 min. Rosettes were removed, and the resulting condensed vapor on the tube walls was collected by centrifugation at 5000 rpm for 3 min. Finally, 1 μL of the collected vapor was placed in a 10-mL headspace sample vial to carry out the full evaporation of the sample at 80°C for 20 min before headspace gas chromatography measurement.

Headspace gas chromatography measurements were done with a TRACE 1300 (Thermo Fisher Scientific) gas chromatograph coupled to a flame ionization detector (FID). The column used was an Rtx-5 w/Integra-Guard (Restek) 30 m long, 0.32 mm i.d., and a film thickness of 0.25 μm. The chromatographic method was modified from Tiscione et al. (2011), using helium as a gas carrier. Run conditions were as follows: inlet 90°C with an split ratio of 5:1, gas carrier flow of 3 mL/min; oven 35°C for 2 min with a ramp of 25°C/min until 90°C, hold for 0.8 min; FID detector at 300°C; hydrogen flow rate of 40 mL/min and air flow rate of 450 mL/min. To test the detection limit of the gas chromatograph-FID, a five-point calibration curve was done with 1.0, 0.5, 0.1, 0.05, and 0.01 ppm methanol. Every point of the calibration curve was measured in triplicate with 5 min total time per run.

Preparation of Alcohol-Insoluble Residues

Plant tissue (200 mg) was ground in liquid nitrogen and rinsed three times with 10 mL of 80% (v/v) aqueous ethanol at room temperature for 1 h. Then, lipids were removed by rinsing three times with 1:1 (v/v) methanol: chloroform followed by three rinses with 100% acetone. The final alcohol-insoluble residue (AIR) materials were dried at room temperature by evaporation overnight.

Acid Hydrolysis and Sugar Quantification

Two milligrams of AIR was hydrolyzed for 1 h with 400 μL of 2 M trifluoroacetic acid (TFA) at 121°C. TFA was evaporated at 60°C with nitrogen gas, and samples were washed twice with 400 μL of isopropanol and then dried with nitrogen gas. Hydrolyzed samples were suspended in 1 mL of deionized water, sonicated during 15 min, filtered through a syringe filter (pore size, 0.45 μm), and used forHigh-Performance Anion-Exchange Chromatography with Pulsed Amperometric Detection analysis as described below. Inositol and allose were used as the internal controls for TFA hydrolysis.

A Dionex ICS3000 ion chromatography system, equipped with a pulsed amperometric detector, a CarboPac PA1 (4 × 250 mm) analytical column, and a CarboPac PA1 (4 × 50 mm) guard column, was used to quantify sugars. The separation of neutral sugars was performed at 40°C with a flow rate of 1 mL/min using an isocratic gradient of 20 mM NaOH for 20 min followed by a wash with 200 mM NaOH for 10 min. After every run, the column was equilibrated in 20 mM NaOH for 10 min. Separation of acidic sugars was performed using 150 mM NaOAc and 100 mM NaOH for 10 min at a flow rate of 1 mL/min at 40°C. Standard curves of neutral sugars (D-Fuc, L-Rha, L-Ara, D-Gal, D-Glc, D-Xyl, and D-Man) or acidic sugars (D-GalA and D-GlcA) were used for quantification.

Determination of HG Epitope Abundance by ELISA

Samples (5 mg) of leaf AIR materials (see above) were sequentially extracted with 2 mL of water, cyclohexylenedinitrilotetraacetate, KOH, and cellulose as described elsewhere (Wang et al., 2019) to generate soluble fractions containing HG. Extracts were sequentially diluted onto microtiter plates and incubated overnight at 4°C. Plates were then washed vigorously with tap water six times and shaken dry. Microtiter plate wells were blocked using 200 μL per well of milk-PBS (5%, 1×) for 2 h at room temperature. The plates were washed nine times in tap water and shaken dry. Primary HG-directed antibodies (LM19 and LM20) were added at 100 μL per well as 10-fold dilutions of hybridoma cell culture supernatants in milk-PBS (5%, 1×) and incubated for 1 h. In the case of 2F4, a Tris-based saline buffer was

used and the hybridoma supernatant was diluted 200-fold. Plates were washed nine times in tap water and shaken dry before the secondary antibody incubation. Secondary antibodies (anti-rat or anti-mouse horseradish peroxidase-conjugated IgG; Sigma-Aldrich) were added at 100 μL per well at 1000-fold dilution in milk-PBS (5%, 1×) for 1 h at room temperature. After extensive washing in tap water, microtiter plates were developed using 100 μL of substrate per well (0.1 M sodium acetate buffer, pH 6, 1% 3,3,5′5′-tetramethylbenzidine, and 0.006% H_2O_2). The enzyme reaction was stopped by the addition of 50 μL of 2.5 M H_2SO_4 to each well, and the absorbance of each well at 450 nm was determined.

Determination of HG Degree of Methylesterification

One milligram of AIR was mixed with 100 μL of deionized water in 1.5-mL tubes, and HG methyl groups were released by alkali treatment by adding 100 μL of 1 M NaOH during 1 h at 4°C. Reactions were neutralized by adding 100 μL of 1 M HCl. In a separate 2-mL tube, methanol oxidation by alcohol oxidase was performed by mixing 100 μL of 200 mM Tris-HCl buffer, pH 7.5, 40 μL of 3 mg/mL *N*-methylbenzothiazolinone-2-hydrazone, 25 μL of the previously demethylesterified sample, and 20 μL of 0.02 units/μL alcohol oxidase. After a brief vortex, the reaction mix was incubated for 20 min at 30°C. Colorimetric reactions were started by incorporation of 200 μL of sulfamic acid/ferric ammonium sulfate (0.5% [w/v] with deionized water), a brief vortex, and incubation for 20 min at room temperature. Finally, 600 μL of deionized water was added, and absorbance was measured at 620 nm. Results were expressed as μmol of methanol released per g of AIR.

Tissue Processing, Embedding, and Sectioning

After infestation treatments, rosette leaves were stored in FAA fixative solution (3.7% formaldehyde, 5% glacial acetic acid, and 50% ethanol) for at least 2 weeks at 4°C. Fixed tissue was dehydrated by serial incubations at 4°C in solutions with an increasing concentration of ethanol from 10% to 100%. LR White resin (Sigma-Aldrich) was infiltrated into the tissue by incubations at 4°C in serial solutions with increasing concentrations of resin (100% ethanol:LR White, from 4:1 to 1:4) plus two overnight infiltrations with pure resin at room temperature. Once infiltrated, tissues were placed into hard gelatin capsules, submerged in resin, and polymerized at 50°C for 24 h. One-micrometer sections were obtained from resin blocks with a rotatory micrometer and placed on glass slides pretreated with Vectabond (Vector Laboratories) for immunofluorescence assays.

Immunofluorescence and Confocal Microscopy

LM19 and LM20 rat monoclonal antibodies were used to target unesterified and highly methylesterified HGs, respectively (Verhertbruggen et al., 2009). Additionally, the 2F4 mouse antibody was used to target egg box epitopes formed due to the dimeric association of unesterified HG chains through calcium ions (Liners et al., 1989; Liners and Van Cutsem, 1992). Slides with sections were incubated for 30 min at room temperature with 5% fat-free milk (Svelty) dissolved in 1× PBS to block nonspecific binding sites and washed once with 1× PBS. Primary antibody diluted 1:5 in milk-PBS (5%, 1×) was added and incubated at room temperature for 90 min. Three washes with 1× PBS were done before incubation with the secondary antibody. Alexa Fluor 488 goat anti-rat or anti-mouse antibody (Life Technologies) was diluted 1:100 in milk-PBS (5%, 1×) and incubated with sections at room temperature for 60 min. Samples were then washed three times with 1× PBS. A solution of 0.25 mg/mL Calcofluor White (Sigma-Aldrich) in 1× PBS was added for 5 min to stain all cell walls. Two washes with 1× PBS were performed, and the anti-fade agent Citifluor (Agar Scientific) was added before cover slip mounting. Images were taken with a Leica TCS LSI confocal microscope with a PlanApo 5×/0.5 LWD objective lens. Immunolabeling of different conditions was done at least in triplicate, and the most representative image of the corresponding batch was chosen.

Quantification of Immunofluorescence Signal

Antibody and Calcofluor White signal areas were measured with ImageJ software. Each image was transformed to a eight-bit image, and the threshold was adjusted for each channel (Calcofluor White and Alexa Fluor 488) using the same threshold parameters for all biological replicates. Then, signal areas were selected with the option "create selection" and measured with the menu tool "measure." For each image, the area of antibody signal was measured and represented as percentage with respect to the total cell wall area (Calcofluor White signal). Then, measures obtained for the infested condition were normalized to the control condition (non-infested) assigned as 100%. Compared images (i.e., infested versus noninfested slices) correspond to samples obtained from the same plant culture batch and within the same immunofluorescence experiment.

Cloning of *PMEI13*

The *PMEI13* coding sequence was cloned using cDNA synthesized from Arabidopsis leaf RNA as a template. Sequences without the signal peptide were PCR-amplified using *Pfu*Ultra II fusion HS DNA polymerase (Agilent) and the following primer pair: FWPMEI13NP (5′-CACCACAACAACAACAA CTACAA-3′ and 5′-TTAGCCATGAATAGAAGCAAAGTG-3′). Resulting PCR products were inserted into the pENTR/D-TOPO cloning vector according to the standard protocol (Thermo Fisher Scientific) to generate the entry clone pENTR-PMEI13NP. The C-terminal His_6 fusion was obtained by recombining the entry clones pENTR-PMEI13NP with the destination vector Champion pET300/NT-DEST using LR clonase (Thermo Fisher Scientific). *Escherichia coli* strain BL21 (DE3) was subsequently transformed.

Heterologous Expression of *PMEI13* in *E. coli*

E. coli carrying the recombinant PMEI13 (PMEI13-His_6) construct was grown inLuria-Bertani medium with 100 μg/mL ampicillin at 37°C with shaking until OD_{600} of ~0.6. Expression of the fusion protein was induced by the addition of 0.2 mM IPTG and incubation at 37°C for 3 h. The bacterial pellet was harvested by centrifugation. Extraction of proteins was performed by resuspension of this in 50 mM phosphate buffer, pH 7.5, and 100 mM NaCl, followed by sonication. The supernatant was collected by centrifugation, and the protein concentration was determined as described above. Proteins were analyzed by SDS-PAGE using a 12% acrylamide/bis-acrylamide gel and stained with Coomassie Brilliant Blue G 250.

Characterization of PMEI13-Inhibiting Activity

Total protein extract (30 μg) from the different *E. coli* cultures was put in contact with 30 μg of total extract protein of wild-type plants. Then, using a gel diffusion assay, as described by Saez-Aguayo et al. (2013, 2017), the inhibitory effect of recombinant PMEI13 on global PME activity of wild-type plants was determined. PME activity was normalized to the average empty vector (the expression vector without the PMEI13 insert) activity.

Probing and Feeding Behavior of *M. persicae* on Arabidopsis Plants Using the EPG Technique

Once an explorer aphid has landed on a potential host, a complex and integrative evaluation of gustatory, olfactory, and mechanosensory parameters assesses the suitability of the host to establish a new colony (Schoonhoven et al., 2005; Van Emden and Harrington, 2017). This early

host examination step is critical to accept or reject a potential host, and in this way, we defined as the early plant-aphid interaction the time elapsed between aphid landing and the first sustained phloem sap ingestion (>10 min) (Tjallingii and Mayoral, 1992; Schoonhoven et al., 2005). To establish the optimal sampling time related to early-stage plant-aphid interaction, we performed a detailed feeding behavior study of *M. persicae* on Arabidopsis wild-type Col-0, as the reference host, using EPG. Additionally, probing and feeding behavior profiles of wingless adult *M. persicae* aphids were evaluated on 4-week-old wild-type Col-0, wild-type WS4, *pmei13-1*, and *pmei13-2* plants.

EPG consists of an electrical circuit composed of the aphid and the host plant. Once the insect stylets penetrate the host plant, the circuit is closed, and a fluctuating voltage is created depending on the stylet tip position and the activity inside the plant tissues (Figure 1A). This fluctuating voltage creates distinct patterns referred to as EPG waveforms, which in turn are experimentally related to different feeding processes or activities performed by the insect, in our case the aphid *M. persicae* (Figure 1A). Electrical penetration graphs were recorded using a Giga-4 channel DC-EPG and a Giga-8 DC-EPG device with 1 GΩ of input resistance (EPG Systems). The EPG devices were connected to PC computers via a USB analog/digital converter card (DI- 710; DATAQ Instruments). *M. persicae* individuals were immobilized on a pipette tip coupled to a vacuum pump, and an 18.5-μm-diameter gold wire was attached to the aphid dorsum with water-based conductive silver glue paint (EPG Systems). The other end of the gold wire was glued with a droplet of paint to a copper extension wire (2 cm in length), which was inserted into the input of the EPG probe, which in turn was connected to the Giga-4 or Giga-8 device. The EPG circuit was completed by inserting a copper electrode (10 cm length, 2 mm diameter) into the soil of the pot. Aphids were starved for ~1 h to acclimatize between the time of wiring and the beginning of EPG recording. Wired aphids were placed on fully expanded rosette leaves. Probing and feeding behavior was monitored for 8 h for each aphid/plant combination. Plants and aphids were used only once for each EPG recording. EPG signals were acquired and analyzed using Stylet+ software for Windows (EPG Systems).

Analysis of EPG Waveforms

EPG variables were processed using the EPG-Excel Data Workbook version 5.0 developed by the laboratory of A.F. (Sarria et al., 2009). Recordings in which aphids exhibited aberrant behavior (no feeding during the first hour) were discarded.

The EPG waveforms associated with specific stylet tip positions and activities when aphids probe and feed on plants are well characterized (Tjallingii, 1978). Waveform np represents nonprobing behavior (no stylet contact with the leaf tissue), waveform C represents the intercellular stylet pathway where the insects show a cyclic activity of mechanical stylet penetration and secretion of saliva, and waveform pd (potential drops) represents brief (4–12 s) intracellular stylet punctures during the pathway phase (C). Two waveforms related to phloem activity were recorded: waveform E1, which represents salivation into phloem sieve elements at the beginning of the phloem phase, and waveform E2, which is correlated with passive phloem sap uptake from the sieve element. Furthermore, waveform G represents an active intake of xylem sap, and waveform F represents derailed stylet mechanics. The number of waveform events per insect was calculated using the sum of the number of events of a particular waveform divided by the total number of insects under each treatment. The total duration of the waveform event per insect was calculated using the sum of durations of each event of a particular waveform made by each insect that produced that waveform divided by the total number of insects under each treatment.

Free Choice Assays

The choice assay was performed in order to evaluate the aphid settling preference for a specific genotype or treatment.

The influence of PME activity on host choice by *M. persicae* was evaluated by exogenously modulating global PME activity of 4-week-old wild-type Col-0 and then subjecting these plants to a free choice assay. One group of plants was infiltrated with 1 mg/mL EGCG (Sigma-Aldrich), which has been described as a specific chemical inhibitor of total PME activity (Lewis et al., 2008). Then, the second group of plants was infiltrated with 15 units/mL orange peel PME (Sigma-Aldrich). Treated plants, plus the water-infiltrated control group (mock), were then subjected to a free choice assay. One plant of each treatment was placed within the choice arena, consisting of a 10-mm-diameter transparent acrylic platform connecting the three individual plant pots. Thirty wingless adult aphids were released in the middle of the platform, equidistantly from test plants. After 24 h, the total number of aphids per plant was registered. Results were expressed as a percentage of aphid preference, considering the settled aphid as 100%.

The influence of methanol, released during PME reaction, was evaluated on aphid settling behavior by infiltrating a solution of methanol (0.1% [v/v]) into three rosette leaves of 4-week-old wild-type Col-0 plants. Methanol-treated plants along with mock plants were then used in a free choice assay. One plant of each condition was placed within the choice arena. Thirty wingless adult aphids were released in the middle of the platform, equidistantly from both treated plants. After 24 h, the total number of aphids per plant was registered. Results were expressed as a percentage of aphid preference, considering the settled aphid as 100%

The role of PMEI13 during aphid infestation was evaluated in terms of aphid settling behavior by subjecting both *pmei13* mutant lines along with their respective wild-type genotypes to a free choice assay according to Poch et al. (1998). Two mutants and two wild-type plants were placed equidistantly from the center of 19-cm-diameter plates containing Murashige and Skoog medium supplemented with 2% (w/v) sucrose and set with 0.8% (w/v) agar. Free choice tests were done by challenging 3-week-old Arabidopsis plants with 22 wingless adult aphids released right in the center of the choice plates. The number of aphids per plant was registered at 2, 6, 12, and 24 h after release. At least five choice plates were assayed in parallel.

Statistical Analysis

Technical replicates were averaged to give a single value for each biological replicate, and then these values were used to perform Student's *t* test and to calculate the SE. Therefore, Student's *t* test was done with at least three replicates ($n = 3$), which correspond to the average of at least three technical replicates for each biological replicate. Student's *t* test was performed using GraphPad Prism version 5.00 (GraphPad Software).

SE was calculated by dividing the SD (of the biological replicates) by the square root of the number of biological replicates. In the case of EPG results, the Mann-Whitney *U* test was performed using SPSS Statistics, Version 20.0(IBM).

Accession Numbers

The accession numbers of Arabidopsis *pmei13* mutants used in the present work correspond to Salk_035506 (*pmei13-1*) and FLAG_58B07 (*pmei13-2*).

Supplemental Data

Supplemental Figure 1. HG demethylesterification zones in an aphid-infested leaf has different patterns, distribution, and sizes.

Supplemental Figure 2. Early aphid infestation increases the abundance of demethylesterified HG epitopes.

Supplemental Figure 3. Early aphid infestation decreases the abundance of highly methylesterified HG epitopes.

Supplemental Figure 4. Influence of early aphid infestation on HG epitopes and sugar composition in arabidopsis Leaves.

Supplemental Figure 5. Early aphid infestation increases ion cross-linked HG epitopes.

Supplemental Figure 6. Identification of *pmei13* mutant lines and characterization of PMEI13 inhibitory activity.

Supplemental Figure 7. Characterization of *pmei13* mutant phenotypes.

Supplemental Figure 8. *pmei13-1* mutant possesses increased abundance of demethylesterified HG with respect to wild-type Col-0.

Supplemental Figure 9. *pmei13-2* mutant possesses increased abundance of demethylesterified HG with respect to wild-type WS4.

Supplemental Table 1. *M. persicae* feeding behavior is not altered on PMEI6-OE plants.

Supplemental Table 2. Sequences of primers used in this study.

ACKNOWLEDGMENTS

Thanks to Helen North, from de the IJPB-INRA (Versailles, France), for the gift of the PMEI6 overexpresser, wild-type WS4, and *pmei13-2* genotypes. We also thank Michael Handford (Universidad de Chile) for language support. This work was supported by the Fondo Nacional de Desarrollo Científico y Tecnológico (1170259 and 11160787), the Ministry of Education, Government of Chile (PAI 79170136), and Iniciativa Científica Milenio (Instituto Milenio iBio).

AUTHOR CONTRIBUTIONS

F.B.-H., C.S.-S., and S.S.-A. conceived the study and designed the experimental strategy; P.K. and S.E.M. designed and supervised immunolabeling experiments; R.A.C., A.F., and E.G. designed and supervised aphid settling and feeding behavior experiments; J.C.-B. and S.S.-A. cloned and assayed the inhibiting capacity in vitro of PMEI13; J.P.P.-R. and S.S.-A. quantified monosaccharaides by High-Performance Anion-Exchange Chromatography with Pulsed Amperometric Detection; C.S.-S. and M.A.R. quantified methanol; B.R. and I.R. carried out expression analysis by RT-qPCR; C.S.-S. and P.O. carried out the measurements of enzymatic activities; C.S.-S. and E.G. performed statistical analysis; C.S.-S., S.S.-A., and F.B.-H. wrote the article with input from P.K., A.F., E.G., and R.A.C.

Received March 6, 2019; revised April 29, 2019; accepted May 20, 2019; published May 24, 2019.

REFERENCES

Alonso, J.M., et al. (2003). Genome-wide insertional mutagenesis of Arabidopsis thaliana. Science **301:** 653–657.

Baldwin, I.T., Halitschke, R., Paschold, A., Von Dahl, C.C., and Preston, C.A. (2006). Volatile signaling in plant-plant interactions: "Talking trees" in the genomics era. Science **311:** 812–815.

Bethke, G., Grundman, R.E., Sreekanta, S., Truman, W., Katagiri, F., and Glazebrook, J. (2014). Arabidopsis PECTIN METHYLESTERASEs contribute to immunity against *Pseudomonas syringae*. Plant Physiol. **164:** 1093–1107.

Bracccini, I., Grasso, R.P., and Pérez, S. (1999). Conformational and configurational features of acidic polysaccharides and their interactions with calcium ions: A molecular modeling investigation. Carbohydr. Res. **317:** 119–130.

Caffall, K.H., and Mohnen, D. (2009). The structure, function, and biosynthesis of plant cell wall pectic polysaccharides. Carbohydr. Res. **344:** 1879–1900.

Cantu, D., Vicente, A.R., Labavitch, J.M., Bennett, A.B., and Powell, A.L. (2008). Strangers in the matrix: Plant cell walls and pathogen susceptibility. Trends Plant Sci. **13:** 610–617.

Dedryver, C.A., Le Ralec, A., and Fabre, F. (2010). The conflicting relationships between aphids and men: A review of aphid damage and control strategies. C. R. Biol. **333:** 539–553.

De Vos, M., Van Oosten, V.R., Van Poecke, R.M., Van Pelt, J.A., Pozo, M.J., Mueller, M.J., Buchala, A.J., Métraux, J.P., Van Loon, L.C., Dicke, M., and Pieterse, C.M. (2005). Signal signature and transcriptome changes of Arabidopsis during pathogen and insect attack. Mol. Plant Microbe Interact. **18:** 923–937.

Dixit, S., Upadhyay, S.K., Singh, H., Sidhu, O.P., Verma, P.C., and K, C. (2013). Enhanced methanol production in plants provides broad spectrum insect resistance. PLoS One **8:** e79664.

Dorokhov, Y.L., Komarova, T.V., Petrunia, I.V., Frolova, O.Y., Pozdyshev, D.V., and Gleba, Y.Y. (2012). Airborne signals from a wounded leaf facilitate viral spreading and induce antibacterial resistance in neighboring plants. PLoS Pathog. **8:** e1002640.

Dreyer, D.L., and Campbell, B.C. (1987). Chemical basis of host-plant resistance to aphids. Plant Cell Environ. **10:** 353–361.

Fraeye, I., Colle, I., Vandevenne, E., Duvetter, T., Van Buggenhout, S., Moldenaers, P., Van Loey, A., and Hendrickx, M. (2010). Influence of pectin structure on texture of pectin-calcium gels. Innov. Food Sci. Emerg. Technol. **11:** 401–409.

Garzo, E., Soria, C., Gomez-Guillamon, M.L., and Fereres, A. (2002). Feeding behavior of *Aphis gossypii* on resistant accessions of different melon genotypes (*Cucumis melo*). Phytoparasitica **30:** 129–140.

Gramegna, G., Modesti, V., Savatin, D.V., Sicilia, F., Cervone, F., and De Lorenzo, G. (2016). GRP-3 and KAPP, encoding interactors of WAK1, negatively affect defense responses induced by oligogalacturonides and local response to wounding. J. Exp. Bot. **67:** 1715–1729.

Harrewijn, P., and Kayser, H. (1997). Pymetrozine, a fast-acting and selective inhibitor of aphid feeding: In-situ studies with electronic monitoring of feeding behaviour. Pestic. Sci. **49:** 130–140.

Hooks, C.R., and Fereres, A. (2006). Protecting crops from non-persistently aphid-transmitted viruses: A review on the use of barrier plants as a management tool. Virus Res. **120:** 1–16.

Hothorn, M., Wolf, S., Aloy, P., Greiner, S., and Scheffzek, K. (2004). Structural insights into the target specificity of plant invertase and pectin methylesterase inhibitory proteins. Plant Cell **16:** 3437–3447.

Ibar, C., and Orellana, A. (2007). The import of *S*-adenosylmethionine into the Golgi apparatus is required for the methylation of homogalacturonan. Plant Physiol. **145:** 504–512.

Jin, D.F., and West, C.A. (1984). Characteristics of galacturonic acid oligomers as elicitors of casbene synthetase activity in castor bean seedlings. Plant Physiol. **74:** 989–992.

Jolie, R.P., Duvetter, T., Van Loey, A.M., and Hendrickx, M.E. (2010). Pectin methylesterase and its proteinaceous inhibitor: A review. Carbohydr. Res. **345:** 2583–2595.

Kimmins, F.M. (1986). Ultrastructure of the stylet pathway of *Brevicoryne brassicae* in host plant tissue, *Brassica oleracea*. Entomol. Exp. Appl. **41:** 283–290.

Klingler, J., Powell, G., Thompson, G.A., and Isaacs, R. (1998). Phloem specific aphid resistance in *Cucumis melo* line AR 5: Effects on feeding behaviour and performance of *Aphis gossypii*. Entomol. Exp. Appl. **86:** 79–88.

Klingler, J., Creasy, R., Gao, L., Nair, R.M., Calix, A.S., Jacob, H.S., Edwards, O.R., and Singh, K.B. (2005). Aphid resistance in *Medicago truncatula* involves antixenosis and phloem-specific, inducible antibiosis, and maps to a single locus flanked by NBS-LRR resistance gene analogs. Plant Physiol. **137:** 1445–1455.

Komarova, T.V., Sheshukova, E.V., and Dorokhov, Y.L. (2014). Cell wall methanol as a signal in plant immunity. Front. Plant Sci. **5:** 101.

Le Roux, V., Dugravot, S., Campan, E., Dubois, F., Vincent, C., and Giordanengo, P. (2008). Wild Solanum resistance to aphids: Antixenosis or antibiosis? J. Econ. Entomol. **101:** 584–591.

Levesque-Tremblay, G., Pelloux, J., Braybrook, S.A., and Müller, K. (2015). Tuning of pectin methylesterification: Consequences for cell wall biomechanics and development. Planta **242:** 791–811.

Lewis, K.C., Selzer, T., Shahar, C., Udi, Y., Tworowski, D., and Sagi, I. (2008). Inhibition of pectin methyl esterase activity by green tea catechins. Phytochemistry **69:** 2586–2592.

Liners, F., and Van Cutsem, P. (1992). Distribution of pectic polysaccharides throughout walls of suspension-cultured carrot cells. Protoplasma **170:** 10–21.

Liners, F., Letesson, J.J., Didembourg, C., and Van Cutsem, P. (1989). Monoclonal antibodies against pectin: Recognition of a conformation induced by calcium. Plant Physiol. **91:** 1419–1424.

Lionetti, V., Fabri, E., De Caroli, M., Hansen, A. R., Willats, W. G., Piro, G., and Bellincampi, D. (2017). Three pectin methyl esterase inhibitors protect cell wall integrity for immunity to Botrytis. Plant Physiol.**173:** 1844–1863.

Ma, R., Reese, J.C., Black, W.C., IV, and Bramel-Cox, P. (1990). Detection of pectinesterase and polygalacturonase from salivary secretions of living greenbugs, *Schizaphis graminum* (Homoptera: Aphididae). J. Insect Physiol. **36:** 507–512.

Malinovsky, F.G., Fangel, J.U., and Willats, W.G. (2014). The role of the cell wall in plant immunity. Front. Plant Sci. **5:** 178.

McAllan, J.W., and Adams, J.B. (1961). The significance of pectinase in plant penetration by aphids. Can. J. Zool. **39:** 305–310.

Murray, D.A., Clarke, M.B., and Ronning, D.A. (2013). Estimating invertebrate pest losses in six major Australian grain crops. Aust. J. Entomol. **52:** 227–241.

Navazio, L., Moscatiello, R., Bellincampi, D., Baldan, B., Meggio, F., Brini, M., Bowler, C., and Mariani, P. (2002). The role of calcium in oligogalacturonide-activated signalling in soybean cells. Planta **215:** 596–605.

Ngouémazong, D.E., Tengweh, F.F., Fraeye, I., Duvetter, T., Cardinaels, R., Van Loey, A., Moldenaers, P., and Hendrickx, M. (2012). Effect of de-methylesterification on network development and nature of Ca^{2+} pectin gels: Towards understanding structure-function relations of pectin. Food Hydrocoll. **26:** 89–98.

North, H.M., De Almeida, A., Boutin, J.P., Frey, A., To, A., Botran, L., Sotta, B., and Marion-Poll, A. (2007). The Arabidopsis ABA-deficient mutant aba4 demonstrates that the major route for stress-induced ABA accumulation is via neoxanthin isomers. Plant J. **50:** 810–824.

Osorio, S., Castillejo, C., Quesada, M.A., Medina-Escobar, N., Brownsey, G.J., Suau, R., Heredia, A., Botella, M.A., and Valpuesta, V. (2008). Partial demethylation of oligogalacturonides by pectin methyl esterase 1 is required for eliciting defence responses in wild strawberry (*Fragaria vesca*). Plant J. **54:** 43–55.

Östman, Ö., Ekbom, B., and Bengtsson, J. (2003). Yield increase attributable to aphid predation by ground-living polyphagous natural enemies in spring barley in Sweden. Ecol. Econ. **45:** 149–158.

Peaucelle, A., Louvet, R., Johansen, J.N., Höfte, H., Laufs, P., Pelloux, J., and Mouille, G. (2008). Arabidopsis phyllotaxis is controlled by the methyl-esterification status of cell-wall pectins. Curr. Biol. **18:** 1943–1948.

Peaucelle, A., Braybrook, S.A., Le Guillou, L., Bron, E., Kuhlemeier, C., and Höfte, H. (2011). Pectin-induced changes in cell wall mechanics underlie organ initiation in Arabidopsis. Curr. Biol. **21:** 1720–1726.

Peng, H.C., and Walker, G.P. (2018). Sieve element occlusion provides resistance against *Aphis gossypii* in TGR-1551 melons. Insect Sci.10.1111/1744-7917.12610

Poch, H.L.C., Ponz, F., and Fereres, A. (1998). Searching for resistance in *Arabidopsis thaliana* to the green peach aphid *Myzus persicae*. Plant Sci. **138:** 209–216.

Raiola, A., Lionetti, V., Elmaghraby, I., Immerzeel, P., Mellerowicz, E.J., Salvi, G., Cervone, F., and Bellincampi, D. (2011). Pectin methylesterase is induced in Arabidopsis upon infection and is necessary for a successful colonization by necrotrophic pathogens. Mol. Plant Microbe Interact. **24:** 432–440.

Ridley, B.L., O'Neill, M.A., and Mohnen, D. (2001). Pectins: Structure, biosynthesis, and oligogalacturonide-related signaling. Phytochemistry **57:** 929–967.

Saez-Aguayo, S., et al. (2017). UUAT1 is a Golgi-localized UDP-uronic acid transporter that modulates the polysaccharide composition of Arabidopsis seed mucilage. Plant Cell **29:** 129–143.

Saez-Aguayo, S., Ralet, M.C., Berger, A., Botran, L., Ropartz, D., Marion-Poll, A., and North, H.M. (2013). PECTIN METHYLESTERASE INHIBITOR6 promotes Arabidopsis mucilage release by limiting methylesterification of homogalacturonan in seed coat epidermal cells. Plant Cell **25:** 308–323.

Sarria, E., Cid, M., Garzo, E., and Fereres, A. (2009). Excel Workbook for automatic parameter calculation of EPG data. Comput. Electron. Agric. **67:** 35–42.

Schoonhoven, L.M., Van Loon, B., van Loon, J.J., and Dicke, M. (2005). Insect-Plant Biology. (Oxford, UK: Oxford University Press).

Sénéchal, F., Mareck, A., Marcelo, P., Lerouge, P., and Pelloux, J. (2015). Arabidopsis PME17 activity can be controlled by Pectin Methylesterase Inhibitor4. Plant Signal. Behav. **10:** e983351.

Tiscione, N.B., Alford, I., Yeatman, D.T., and Shan, X. (2011). Ethanol analysis by headspace gas chromatography with simultaneous flame-ionization and mass spectrometry detection. J. Anal. Toxicol. **35:** 501–511.

Tjallingii, W.F. (1978). Electronic recording of penetration behaviour by aphids. Entomol. Exp. Appl. **24:** 721–730.

Tjallingii, W.F. (2006). Salivary secretions by aphids interacting with proteins of phloem wound responses. J. Exp. Bot. **57:** 739–745.

Tjallingii, W.F., and Esch, T.H. (1993). Fine structure of aphid stylet routes in plant tissues in correlation with EPG signals. Physiol. Entomol. **18:** 317–328.

Tjallingii, W.F., and Mayoral, A. (1992). Criteria for host-plant acceptance by aphids. In Proceedings of the 8th International Symposium on Insect-Plant Relationships, S.B.J. Menken, J.H. Visser, and P. Harrewijn, eds (Dordrecht, The Netherlands: Springer), pp. 280–282.

Uluisik, S., Chapman, N.H., Smith, R., Poole, M., Adams, G., Gillis, R.B., Besong, T.M., Sheldon, J., Stiegelmeyer, S., Perez, L., Samsulrizal, N., and Wang, D., et al. (2016) Genetic improvement of tomato by targeted control of fruit softening. Nat. Biotechnol. **34:** 950–952.

Van Emden, H.F., and Harrington, R. (2017). Aphids as Crop Pests. (Wallingford: CABI).

Verhertbruggen, Y., Marcus, S.E., Haeger, A., Ordaz-Ortiz, J.J., and Knox, J.P. (2009). An extended set of monoclonal antibodies to pectic homogalacturonan. Carbohydr. Res. **344:** 1858–1862.

von Dahl, C.C., Hävecker, M., Schlögl, R., and Baldwin, I.T. (2006). Caterpillar-elicited methanol emission: A new signal in plant-herbivore interactions? Plant J. **46:** 948–960.

Wang, D., et al. (2019). Characterization of CRISPR mutants targeting genes modulating pectin degradation in ripening tomato. Plant Physiol. **179:** 544–557.

Willats, W.G., Orfila, C., Limberg, G., Buchholt, H.C., van Alebeek, G.J.W., Voragen, A.G., Marcus, S.E., Christensen, T.M., Mikkelsen, J.D., Murray, B.S., and Knox, J.P. (2001). Modulation of the degree and pattern of methyl-esterification of pectic homogalacturonan in plant cell walls: Implications for pectin methyl esterase action, matrix properties, and cell adhesion. J. Biol. Chem. **276:** 19404–19413.

Wolf, S., and Greiner, S. (2012). Growth control by cell wall pectins. Protoplasma **249** (suppl. 2): S169–S175.

Wolf, S., Mouille, G., and Pelloux, J. (2009). Homogalacturonan methyl-esterification and plant development. Mol. Plant **2:** 851–860.

Zhang, C., Shi, H., Chen, L., Wang, X., Lü, B., Zhang, S., Liang, Y., Liu, R., Qian, J., Sun, W., You, Z., and Dong, H. (2011). Harpin-induced expression and transgenic overexpression of the phloem protein gene AtPP2-A1 in Arabidopsis repress phloem feeding of the green peach aphid *Myzus persicae*. BMC Plant Biol. **11:** 11.